Mid-Infrared Bloch Surface Waves for biosensing applications

Raffaella Polito[1], Agostino Occhicone[1], Marialilia Pea[2], Valeria Giliberti[3], Alberto Sinibaldi[1], Francesco Mattioli[2], Sara Cibella[2], Andrea Notargiacomo[2], Alessandro Nucara[1], Paolo Biagioni[4], Francesco Michelotti[1], Michele Ortolani[1], and Leonetta Baldassarre[1]

[1]*Sapienza University of Rome, Rome, 00185 Italy*
[2]*CNR – Institute for Photonics and Nanotechnologies, Rome, 00156 Italy*
[3]*Center for Life Nanosciences – Istituto Italiano di Tecnologia, Rome, 00161 Italy*
[4]*Politecnico di Milano, Milano, 20133 Italy*

Mid-Infrared Bloch Surface Waves for biosensing applications

Raffaella Polito[1], Agostino Occhicone[1], Marialilia Pea[2], Valeria Giliberti[3], Alberto Sinibaldi[1], Francesco Mattioli[2], Sara Cibella[2], Andrea Notargiacomo[2], Alessandro Nucara[1], Paolo Biagioni[4], Francesco Michelotti[1], Michele Ortolani[1], and Leonetta Baldassarre[1]

[1]Sapienza University of Rome, Rome, 00185 Italy
[2]CNR – Institute for Photonics and Nanotechnologies, Rome, 00154 Italy
[3]Center for Life Nanosciences – Istituto Italiano di Tecnologia, Rome, 00161 Italy
[4]Politecnico di Milano, Milano, 20133 Italy

Abstract— We report on the design, fabrication, and spectroscopic characterization of a 1D Photonic Cristal (1DPC) sustaining Bloch Surface Waves (BSWs) in the mid-infrared. The reported all-dielectric 1DPC structure shows potential for **label-free biosensing applications to medical diagnostics.**

I. INTRODUCTION

Mid-Infrared (MIR) spectroscopy could play a relevant role in the field of label-free biosensors for medical diagnostics thanks to the molecular specificity of vibrational fingerprints in the infrared and terahertz spectral region. Nevertheless, the long wavelength and the low sensitivity of detectors in the MIR if compared to the VIS/NIR range prevent the application to very thin biolayers for the investigation of the mutual interactions between biomolecules, e.g. antibody/antigen or antibody/membrane proteins. Surface plasmon polariton (SPP)-assisted biosensors are exploited in biosensing due to the strongly enhanced field at the metal-dielectric interface, localized in sub-wavelength volumes [1]. In the MIR spectral region, however, SPPs suffer from an extremely poor field confinement, because metals behave almost as perfect conductors in the MIR.

A promising alternative to SPP-based sensors in the mid-IR could be represented by Bloch surface wave (BSW)-based biosensors. BSWs are electromagnetic modes sustained at the interface between a homogeneous dielectric medium and a periodic structure made of two dielectric media of alternating high/low refractive index (one-dimensional photonic crystal, 1DPC). These modes are evanescent waves penetrating both inside the 1DPC and into the homogeneous external medium and their dispersion relations are located within the photonic bandgap where the propagation of specific wavelengths is blocked. BSWs have been largely employed in the VIS/NIR range [2] but only initial demonstration has been provided in the MIR [3]. The 1DPC, deposited on top of a IR-transparent prism, can sustain such propagating surface modes when excited in the Kretschmann-Raether configuration.

II. RESULTS

We have designed, deposited and characterized a 1DPC structure consisting of a periodic structure of two ZnS/CaF_2 pairs [4]. By tuning the layers thickness, our 1DPC operates at wavelength around λ_0=5.6 μm corresponding to the main absorption peaks of proteins (amide-I).

Dielectric media were directly deposited onto custom CaF_2 prisms by thermal evaporation under high vacuum. In order to have the largest possible photonic bandgap, ZnS was selected as the dielectric material with high refractive index (n_{ZnS}=2.24 at λ_0=5.6 μm), while CaF_2 as the low refractive index one ($n_{CaF2} \simeq 1.39$ at λ_0=5.6 μm) because it is characterized by a high IR transparency up to $\lambda = 10$ μm (ZnS is transparent up to $\lambda = 12$ μm) and is almost insoluble in water. Moreover, CaF_2 grows in columnar form under thermal deposition and the resulting voids determine an even lower effective index, i.e. an even wider photonic bandgap. The fabricated final structure was formed starting from top to bottom of ZnS (200nm)/CaF_2 (2250nm)/ZnS (900nm)/CaF_2 (2300nm)/ZnS (890nm)/CaF_2 (adlayer)/CaF_2 substrate. The thin ZnS surface layer on top is referred to as a "defect" layer and is functional to fine-tune the BSW dispersion. The defect layer pushes the BSW states as close as possible to the bandgap center and thus favors a better surface localization of the BSW modes, i.e. a smaller full width at half maximum of experimental reflectance dips.

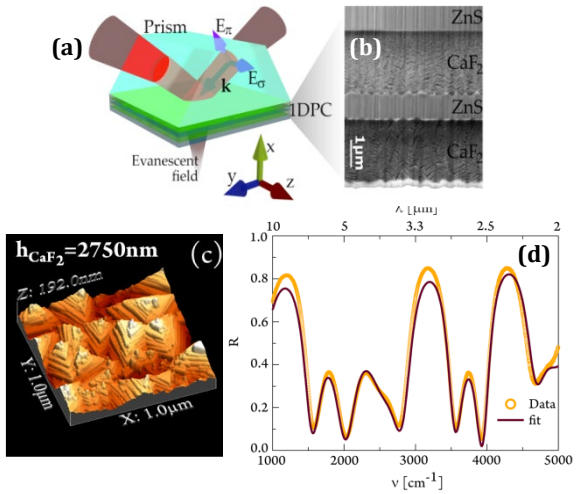

Fig. 1. (a) Pictorial sketch of the photonic crystal deposited on the CaF_2 prism. The IR beam impinges on the 1DPC with an incidence angle θ (Kretschmann-Raether configuration). (b) Cross-sectional scanning electron microscopy picture of the 1DPC. (c) An AFM image (1×1 μm^2) of a 2750 nm-tick CaF_2 layer grown by thermal deposition. The lamellar arrangement and the resulting voids are clearly visible. (d) IR reflection spectrum of the 1DPC (orange dot curve) compared with the corresponding fit curve (red solid curve) obtained with a simplified Fresnel multilayer model. The effective refractive index of CaF_2 retrieved through fitting procedure is $n_{CaF2} = 1.20 \pm 0.04$ at λ_0=5.6 μm.

We performed a morphological characterization of 1DPC inner structure in order to verify the stack quality of the multilayers. Both cross-sectional electron microscopy (SEM)

and atomic force microscopy images confirmed a lamellar arrangement of the deposited CaF_2, further organized into columns oriented along the growth direction (Figure 1b,c). The evaporated structure was also characterized by normal-incidence IR reflectance measurements to retrieve the effective refractive index of CaF_2 through a fitting procedure with a simplified Fresnel multilayer model (the refractive index of CaF_2 after thermal deposition has been evaluated equal to 1.20 ± 0.04 at λ_0=5.6 μm) (Figure 1d).

The 1DPC structure was optimized by means of numerical simulations carried out with the transfer matrix method (TMM). The multilayer, designed in order to maximize the resonant BSW field at the 1DPC/vacuum interface and the BSW bandwidth, is able to sustain BSWs in the wavelength range between 3 and 8 μm.

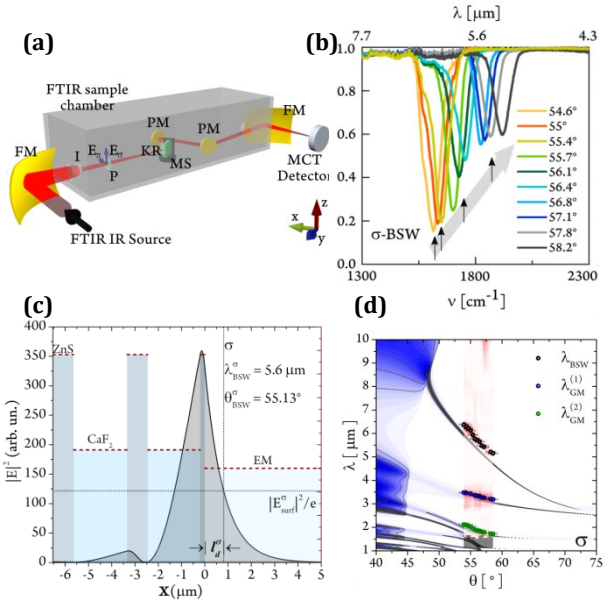

Fig. 2. (a) Pictorial sketch of the optical setup used to excite BSWs: the incoming IR beam, focused by a mirrors system (FM), narrowed by an iris (I) and polarized by a wire-grid polarizer (P) impinges on the 1DPC in KR configuration with an incidence angle that can be controlled remotely with the use of a rotational motorized stage (MS). The outgoing IR beam is eventually focused onto an MCT photovoltaic detector. (b) σ-BSW spectral features between ν =1300 cm^{-1} and 2300 cm^{-1} obtained as described in (a) clearly show a red-shifting in frequency as θ is decreased. (c) Square modulus of the electric field along the direction x perpendicular to the surface. When the incident angle is θ^{σ}_{BSW}= 55.13°, the σ-BSW is exited at 5.6 μm showing a penetration distance (l^{σ}_{d}) of ≃810 nm and a field enhancement (fe) of ~90. The dashed red lines indicate the refractive index profile of the 1DPC. (d) Experimental dispersion of σ-BSWs (black dots) superimposed to the simulated reflectivity map in blue. The blue and green dots correspond to the experimental dispersion of other guided modes (GM) confined mainly within the multilayer structure.

In order to measure the mid-IR spectra of our 1DPC excited in the Kretschmann-Raether (KR) configuration, we have built a custom variable-incidence angle setup with quasi-collimated beam illumination in the sample compartment of a commercial FT-IR spectrometer (Bruker Vertex 70v) (Figure 2a). We have observed clear spectroscopic evidence of BSWs excitation for both transverse electric (σ) and transverse magnetic (π) polarization in the MIR. Figure 2b shows the reflectance dips that we ascribe to σ-BSWs. They show the theoretically expected trend, i.e. a red-shifting in frequency between 1550 and 1900 cm^{-1} (corresponding to wavelength ranging between 6.5 and 5.3 μm) as θ is decreased. In figure 2d the good agreement between our experimental results (red map) with the numerical model (blue map) is demonstrated. The structure is optimized in order to operate at a wavelength around λ_0=5.6 μm and in Figure 2c the theoretical square modulus of the electric inside the 1DPC structure is shown when the σ-BSW is excited in the KR configuration. At λ_0=5.6 μm, the σ-BSW is excited at a resonant angle of θ^{σ}_{BSW} = 55.13° resulting in a penetration distance of the electric field into the external medium of $l^{\sigma}_{d} \simeq 810$ nm. The field enhancement (fe), evaluated as the ratio between the electromagnetic field intensity in vacuum with and without ($|E^{\sigma}_{surf}|^2$) /$|E_0|^2$) the 1DPC, is calculated to be about 90.

The low penetration distance, i.e. high field confinement - l^{σ}_{d}~810 nm instead of several micrometers such as SPPs supported by noble metals in the mid-IR - together with the long field propagation lengths at the 1DPC/external medium interface make BSW-based biosensors good candidates for label-free polarization-dependent sensing devices [4].

III. Summary

In conclusion, MIR BSW biosensors would present several advantages with respect to those based on SPPs due to the intrinsic large field confinement that increases the surfaces sensitivity. Moreover, at variance with SPPs, BSWs can be both σ and π polarized leading to the possibility to perform polarization-resolved vibrational sensing, which is essential to probe protein orientation. Our result show that BSWs are a promising technology for use in future medical devices.

References

[1] F. Neubrech, A. Pucci, T.W. Cornelius, S. Karim, A. García-Etxarri, J. Aizpurua. "Resonant Plasmonic and Vibrational Coupling in a Tailored Nanoantenna for Infrared Detection" *Phys. Rev. Lett.* 101, 157403 (2008).

[2] E. Descrovi, T. Sfez, M. Quaglio, D. Brunazzo, L. Dominici, F. Michelotti, H.P. Herzig, O. Martin, and F. Giorgis. "Guided Bloch Surface Waves on Ultrathin Polymeric Ridges" *Nano Lett.* 10, 2087–2091 (2010).

[3] G. M. Smolik, N. Descharmes, and H. P. Herzig "Toward Bloch Surface Wave-Assisted Spectroscopy in the Mid-Infrared Region" *ACS Photonics* 5, 1164−1170 (2018).

[4] A. Occhicone, M. Pea, R. Polito, V. Giliberti, A. Sinibaldi, F. Mattioli, S. Cibella, A. Notargiacomo, A. Nucara, P. Biagioni, F. Michelotti, M. Ortolani, and L. Baldassarre, Spectral Characterization of Mid-Infrared Bloch Surface Waves Excited on a Truncated 1D Photonic Crystal, *ACS Photonics* 2021 8 (1), 350-359 (2020).